



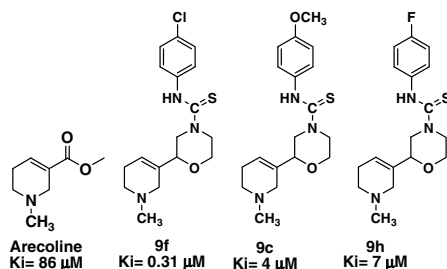
## Bioorganic & Medicinal Chemistry Vol. 16, No. 15, 2008

### Contents

#### ARTICLES

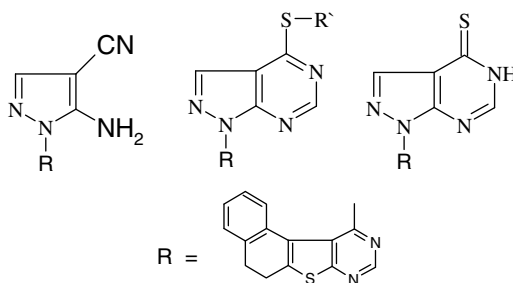
- Muscarinic receptor 1 agonist activity of novel *N*-arylthioureas substituted 3-morpholino arecoline derivatives in Alzheimer's presenile dementia models** pp 7095–7101

Manish Malviya, Y. C. Sunil Kumar, D. Asha, J. N. Narendra Sharath Chandra, M. N. Subhash, K. S. Rangappa\*



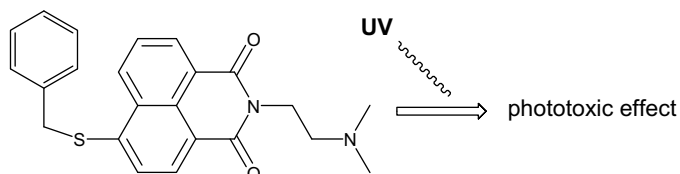
- Synthesis and antiviral evaluation of some new pyrazole and fused pyrazolopyrimidine derivatives** pp 7102–7106

Aymn E. Rashad\*, Mohamed I. Hegab, Randa E. Abdel-Megeid, Jehan A. Micky, Farouk M. E. Abdel-Megeid



- Sulfur-substituted naphthalimides as photoactivatable anticancer agents: DNA interaction, fluorescence imaging, and phototoxic effects in cultured tumor cells** pp 7107–7116

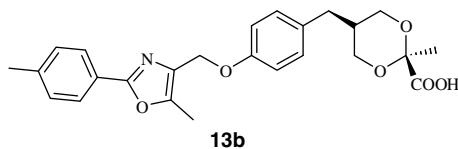
Ingo Ott\*, Yufang Xu, Jianwen Liu, Malte Kokoschka, Melanie Harlos, William S. Sheldrick, Xuhong Qian\*



### Design and synthesis of novel oxazole containing 1,3-Dioxane-2-carboxylic acid derivatives as PPAR $\alpha/\gamma$ dual agonists

pp 7117–7127

Harikishore Pingali\*, Mukul Jain, Shailesh Shah, Pankaj Makadia, Pandurang Zaware, Ashish Goel, Megha Patel, Suresh Giri, Harilal Patel, Pankaj Patel

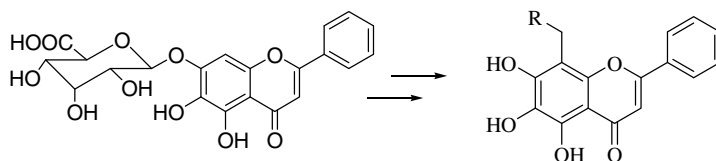


A novel class of PPAR $\alpha/\gamma$  dual agonists containing 1,3-dioxane-2-carboxylic acid was described. Compound **13b** exhibited potent hypoglycemic, hypolipidemic and insulin sensitizing effects in *db/db* mice and Zucker *fa/fa* rats.

### Nitrogen-containing flavonoid analogues as CDK1/cyclin B inhibitors: Synthesis, SAR analysis, and biological activity

pp 7128–7133

Shixuan Zhang\*, Jigang Ma, Yongming Bao, Puwen Yang, Liang Zou, Kangjian Li, Xiaodan Sun

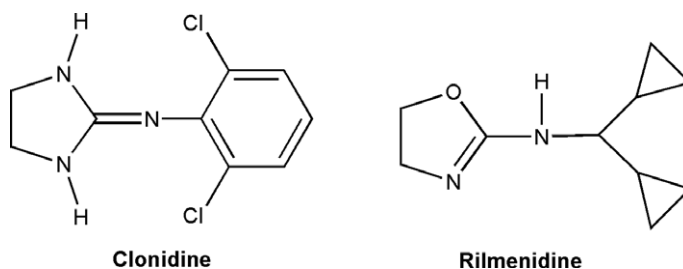


Synthesis and structure–activity relationship of nitrogen-containing flavonoid analogues as CDK1/Cyclin B inhibitors are reported.

### QSAR study of imidazoline antihypertensive drugs

pp 7134–7140

Katarina Nikolic\*, Slavica Filipic, Danica Agbaba



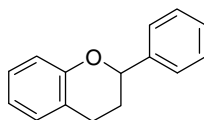
The quantitative structure–activity relationship (QSAR) study of 12 biologically active compounds, including clinically useful clonidine and rilmenidine, was carried out using multilinear regression method on Imidazoline-1 receptor and  $\alpha_2$ -adrenergic receptor binding affinities on human platelets.



### Structure–activity relationship of flavonoids as influenza virus neuraminidase inhibitors and their in vitro anti-viral activities

pp 7141–7147

Ai-Lin Liu, Hai-Di Wang, Simon MingYuen Lee\*, Yi-Tao Wang, Guan-Hua Du\*

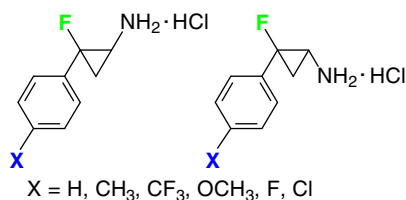


The SAR analysis of flavonoids against influenza virus neuraminidase revealed that for good inhibitory effect, the 4'-OH, 7-OH, C4=O and C2=C3 functionalities were essential.

### Fluorinated phenylcyclopropylamines. Part 5: Effects of electron-withdrawing or -donating aryl substituents on the inhibition of monoamine oxidases A and B by 2-aryl-2-fluoro-cyclopropylamines

pp 7148–7166

Svenja Hruschka, Thomas C. Rosen, Shinichi Yoshida, Kenneth L. Kirk, Roland Fröhlich, Birgit Wibbeling, Günter Haufe\*

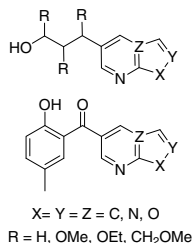


Electron-withdrawing *para*-substituents increase the potency of MAO A inhibition in the *trans*-series, while electron-donating groups have a weak influence on this activity. In contrast, aromatic ring substitution has essentially no effect on inhibition of MAO B. The corresponding *cis*-compounds are 10–100 times less active.

### Synthesis and evaluation of pyrazolo[3,4-*b*]pyridines and its structural analogues as TNF- $\alpha$ and IL-6 inhibitors

pp 7167–7176

Sandip B. Bharate, Tushar R. Mahajan, Yogesh R. Gole, Mahesh Nambiar, T. T. Matan, Asha Kulkarni-Almeida, Sarala Balachandran, H. Junjappa, Arun Balakrishnan, Ram A. Vishwakarma\*

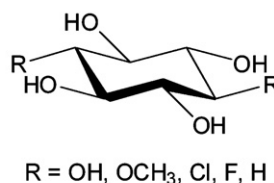
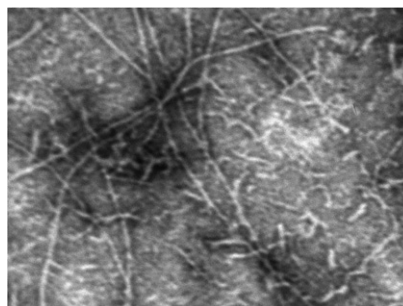


Three different series of pyrazolo[3,4-*b*]pyridines were synthesized and evaluated for their anti-inflammatory activity against TNF- $\alpha$  and IL-6. Several compounds showed promising IL-6 inhibitory activity, amongst which most potent analogue has IC<sub>50</sub> 0.16  $\mu$ M and is not cytotoxic (IC<sub>50</sub> >100  $\mu$ M).

### Synthesis of scyllo-inositol derivatives and their effects on amyloid beta peptide aggregation

pp 7177–7184

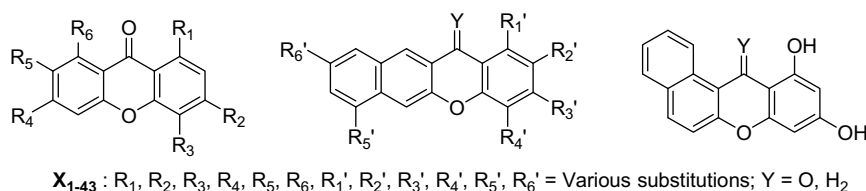
Yedi Sun, Guohua Zhang, Cheryl A. Hawkes, James E. Shaw, JoAnne McLaurin, Mark Nitz\*



### Synthesis, inhibitory activities, and QSAR study of xanthone derivatives as $\alpha$ -glucosidase inhibitors

pp 7185–7192

Yan Liu, Zhuofeng Ke, Jianfang Cui, Wen-Hua Chen, Lin Ma, Bo Wang\*

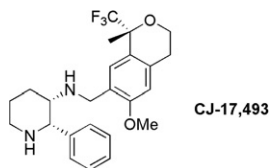


A QSAR model was established by multiple linear regression (MLR) method for a training set of compounds **X<sub>1-34</sub>**. The accuracy and predictive power of the proposed QSAR model were verified by LOO validation, Y-randomization, and test group validation with newly synthesized xanthone derivatives **X<sub>35-43</sub>**.

**Discovery and stereoselective synthesis of the novel isochroman neurokinin-1 receptor antagonist 'CJ-17,493'**

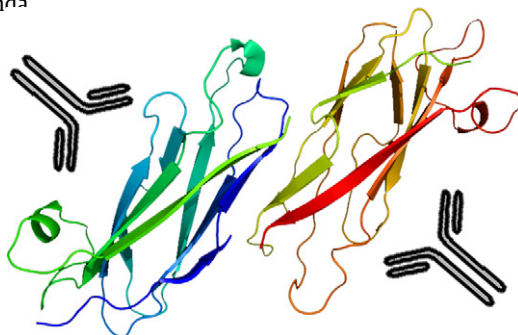
pp 7193–7205

Yuji Shishido\*, Hiroaki Wakabayashi, Hiroki Koike, Naomi Ueno, Seiji Nukui, Tatsuya Yamagishi, Yoshinori Murata, Fumiharu Naganeo, Mayumi Mizutani, Kaoru Shimada, Yoshiko Fujiwara, Ayano Sakakibara, Osamu Suga, Rinko Kusano, Satoko Ueda, Yoshihito Kanai, Megumi Tsuchiya, Kunio Satake

**Major sperm protein as a diagnostic antigen for onchocerciasis**

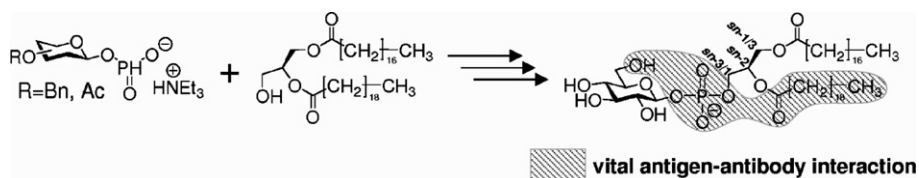
pp 7206–7209

Jungkuk Park, Tobin J. Dickerson\*, Kim D. Jan<sup>da</sup>\*

**Syntheses of phosphatidyl-β-D-glucoside analogues to probe antigen selectivity of monoclonal antibody 'DIM21'**

pp 7210–7217

Peter Greimel, Milaine Lapeyre, Yasuko Nagatsuka, Yoshio Hirabayashi, Yukishige Ito\*

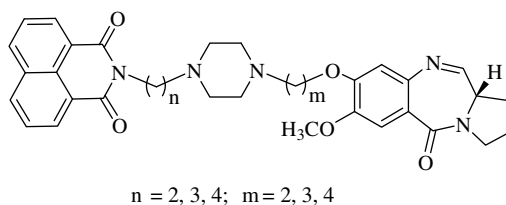


Chemical synthesis of phosphatidyl-β-D-glucoside (PtdGlc) and its analogues was achieved. The proposed structure of natural 6-O-Ac PtdGlc was confirmed. The reactivity of monoclonal antibody 'DIM21' towards PtdGlc and its analogues were mapped.

**Remarkable DNA binding affinity and potential anticancer activity of pyrrolo[2,1-c][1,4]benzodiazepine-naphthalimide conjugates linked through piperazine side-armed alkane spacers**

pp 7218–7224

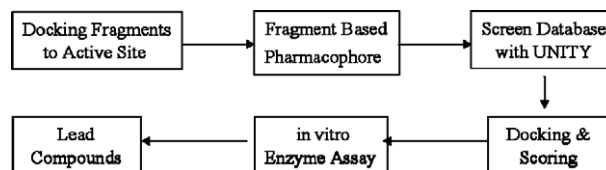
Ahmed Kamal\*, R. Ramu, Venkatesh Tekumalla, G. B. Ramesh Khanna, Madan S. Barkume, Aarti S. Juvekar, Surekha M. Zingde



**Novel inhibitors of anthrax edema factor**

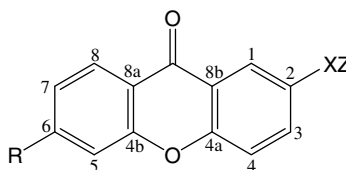
pp 7225–7233

Deliang Chen, Milind Misra, Laurie Sower, Johnny W. Peterson, Glen E. Kellogg, Catherine H. Schein\*

**Anticonvulsant activity of some xanthone derivatives**

pp 7234–7244

Henryk Marona\*, Elżbieta Pękala, Lucyna Antkiewicz-Michaluk, Maria Walczak, Edward Szneler

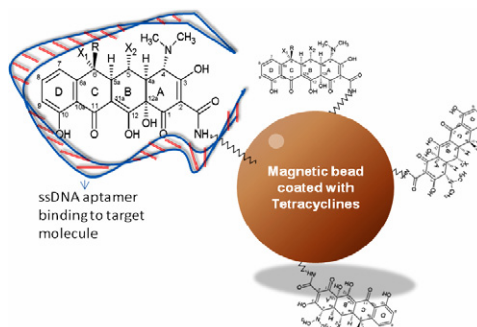


A series of appropriate alkanolamine and amide derivatives of xanthone were prepared and evaluated for anticonvulsant activity using maximal electroshock and subcutaneous pentylenetetrazole-induced seizures, and for neurotoxicity using the rotorod test on mice and rats.

**Single-stranded DNA aptamers specific for antibiotics tetracyclines**

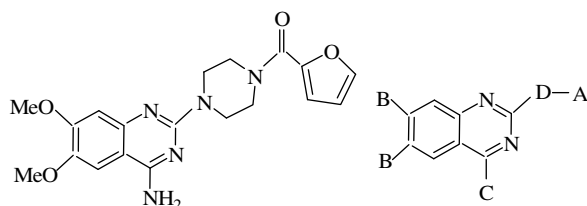
pp 7245–7253

Javed H. Niazi, Su Jin Lee, Man Bock Gu\*

**Molecular features of the prazosin molecule required for activation of Transport-P**

pp 7254–7263

Joaquim Fernando Mendes da Silva, Marcus Walters, Saad Al-Damluji, C. Robin Ganellin\*

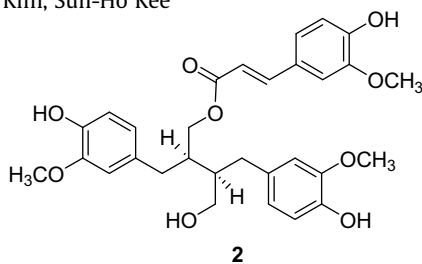
**1** Prazosin

Structural features studied (A-D)

### Hanultarin, a cytotoxic lignan as an inhibitor of actin cytoskeleton polymerization from the seeds of *Trichosanthes kirilowii*

pp 7264–7269

Surk-Sik Moon\*, Aziz Abdur Rahman, Joo-Young Kim, Sun-Ho Kee

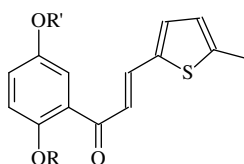


A new lignan derivative, hanultarin, was isolated and structure-determined. It inhibited the polymerization of the actin cytoskeleton and also showed cytotoxic effect against human lung carcinoma A549 and other cell lines.

### Synthesis and cytotoxic, anti-inflammatory, and anti-oxidant activities of 2',5'-dialkoxychalcones as cancer chemopreventive agents

pp 7270–7276

Jen-Hao Cheng, Chi-Feng Hung, Shyh-Chyun Yang\*, Jih-Pyang Wang, Shen-Jeu Won, Chun-Nan Lin\*

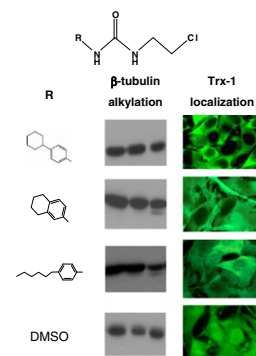


A series of 2',5'-dialkoxychalcones has been synthesized and evaluated their cytotoxic, anti-inflammatory and anti-oxidant activities.

### Selective alkylation of $\beta$ -tubulin and thioredoxin-1 by structurally related subsets of aryl chloroethylureas leading to either anti-microtubules or redox modulating agents

pp 7277–7290

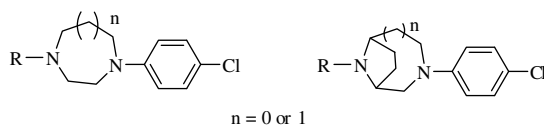
Jessica S. Fortin\*, Marie-France Côté, Jacques Lacroix, Michel Desjardins, Éric Petitclerc, René C.-Gaudreault\*



### Identification of a butyrophenone analog as a potential atypical antipsychotic agent: 4-[4-(4-Chlorophenyl)-1,4-diazepan-1-yl]-1-(4-fluorophenyl)butan-1-one

pp 7291–7301

Seth Y. Ablordeppey\*, Ramazan Altundas, Barbara Bricker, Xue Y. Zhu, Eyunni V. K. Suresh Kumar, Tanise Jackson, Abdul Khan, Bryan L. Roth

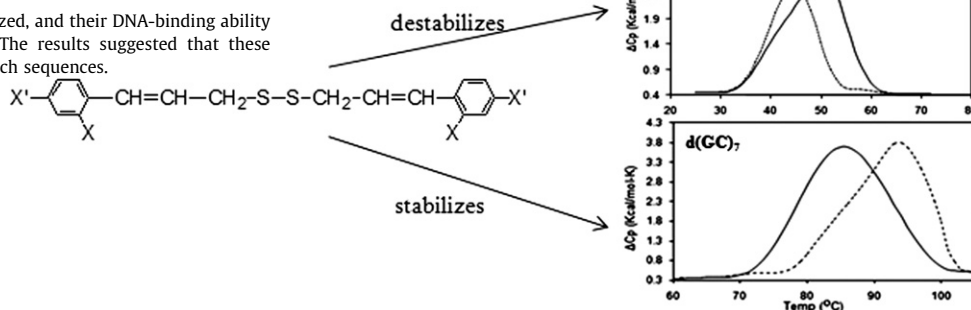


**Synthesis, DNA binding, and cytotoxic evaluation of new analogs of diallyldisulfide, an active principle of garlic**

pp 7302–7310

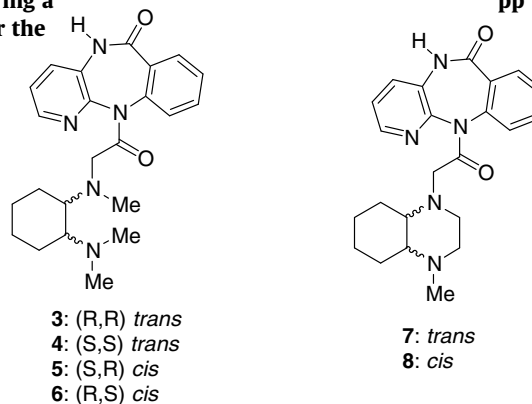
Santosh Kumar Rai,  
Meenakshi Sharma, Manisha Tiwari\*

New analogs of diallyldisulfide were synthesized, and their DNA-binding ability and sequence preferences were evaluated. The results suggested that these analogs have remarkable preference for GC rich sequences.

**Design, synthesis, and biological evaluation of pirenzepine analogs bearing a 1,2-cyclohexanediamine and perhydroquinoxaline units in exchange for the piperazine ring as antimuscarinics**

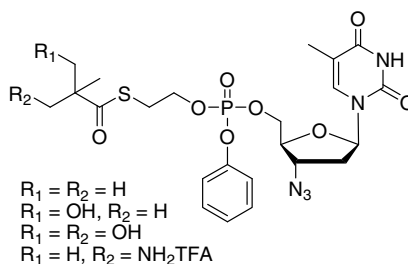
pp 7311–7320

Anna Minarini\*, Gabriella Marucci, Cristina Bellucci, Gianluca Giorgi, Vincenzo Tumiatti, Maria Laura Bolognesi, Riccardo Matera, Michela Rosini, Carlo Melchiorre

**Phenyl phosphotriester derivatives of AZT: Variations upon the SATE moiety**

pp 7321–7329

Anne-Laure Villard, Gaëlle Coussot, Isabelle Lefebvre, Patrick Augustijns, Anne-Marie Aubertin, Gilles Gosselin, Suzanne Peyrottes, Christian Périgaud\*

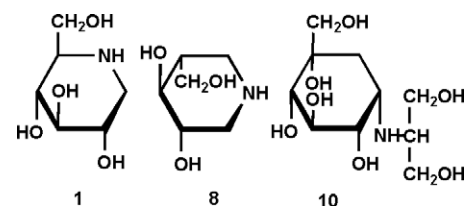


A step further in the SATE mononucleotide prodrug approach.

**In vitro inhibition of glycogen-degrading enzymes and glycosidases by six-membered sugar mimics and their evaluation in cell cultures**

pp 7330–7336

Chinami Kuriyama, Ogusa Kamiyama, Kyoko Ikeda, Fujiko Sanae, Atsushi Kato, Isao Adachi, Tatsushi Imahori, Hiroki Takahata, Tadashi Okamoto, Naoki Asano\*



An amylo-1, 6-glucosidase inhibitor enhanced inhibition of hepatic glucose production in combination with glycogen phosphorylase inhibitor. The inhibitory activity of 1-deoxynojirimycin (1) toward human maltase was identical to that of voglibose (10) of an anti-diabetic agent. L-Isogomine (8), a noncompetitive inhibitor of lysosomal  $\beta$ -glucosidase, also showed a chaperoning activity in N370S Gaucher fibroblasts.

## pp 7337–7346

**Figure 1: Inhibition of cancer cell growth by dGMPi.**

**Left Panel: Molecular Model**

The 3D molecular model shows dGMPi (green sticks) bound to the active site of DNA polymerase beta (grey surface). The following residues are labeled: Asp376, Thr55, Tyr127, Thr415, Asp472, Phe250, Asp32, Asp40, Asp41, Asp42, and Asp43.

**Right Panel: Dose-Response Graph**

The graph plots % inhibition (Y-axis, 0 to 110) against dGMPi concentration [μM] (X-axis, 300 to 160). The data points represent different cancer cell lines, showing a dose-dependent increase in inhibition. The cell lines are: A549, H1299, HCT116, HCT15, HCT19, HCT215, HCT216, HCT219, HCT220, HCT229, HCT230, HCT231, HCT232, HCT233, HCT234, HCT235, HCT236, HCT237, HCT238, HCT239, HCT240, HCT241, HCT242, HCT243, HCT244, HCT245, HCT246, HCT247, HCT248, HCT249, HCT250, HCT251, HCT252, HCT253, HCT254, HCT255, HCT256, HCT257, HCT258, HCT259, HCT260, HCT261, HCT262, HCT263, HCT264, HCT265, HCT266, HCT267, HCT268, HCT269, HCT270, HCT271, HCT272, HCT273, HCT274, HCT275, HCT276, HCT277, HCT278, HCT279, HCT280, HCT281, HCT282, HCT283, HCT284, HCT285, HCT286, HCT287, HCT288, HCT289, HCT290, HCT291, HCT292, HCT293, HCT294, HCT295, HCT296, HCT297, HCT298, HCT299, HCT300, HCT301, HCT302, HCT303, HCT304, HCT305, HCT306, HCT307, HCT308, HCT309, HCT310, HCT311, HCT312, HCT313, HCT314, HCT315, HCT316, HCT317, HCT318, HCT319, HCT320, HCT321, HCT322, HCT323, HCT324, HCT325, HCT326, HCT327, HCT328, HCT329, HCT330, HCT331, HCT332, HCT333, HCT334, HCT335, HCT336, HCT337, HCT338, HCT339, HCT340, HCT341, HCT342, HCT343, HCT344, HCT345, HCT346, HCT347, HCT348, HCT349, HCT350, HCT351, HCT352, HCT353, HCT354, HCT355, HCT356, HCT357, HCT358, HCT359, HCT360, HCT361, HCT362, HCT363, HCT364, HCT365, HCT366, HCT367, HCT368, HCT369, HCT370, HCT371, HCT372, HCT373, HCT374, HCT375, HCT376, HCT377, HCT378, HCT379, HCT380, HCT381, HCT382, HCT383, HCT384, HCT385, HCT386, HCT387, HCT388, HCT389, HCT390, HCT391, HCT392, HCT393, HCT394, HCT395, HCT396, HCT397, HCT398, HCT399, HCT400, HCT401, HCT402, HCT403, HCT404, HCT405, HCT406, HCT407, HCT408, HCT409, HCT410, HCT411, HCT412, HCT413, HCT414, HCT415, HCT416, HCT417, HCT418, HCT419, HCT420, HCT421, HCT422, HCT423, HCT424, HCT425, HCT426, HCT427, HCT428, HCT429, HCT430, HCT431, HCT432, HCT433, HCT434, HCT435, HCT436, HCT437, HCT438, HCT439, HCT440, HCT441, HCT442, HCT443, HCT444, HCT445, HCT446, HCT447, HCT448, HCT449, HCT450, HCT451, HCT452, HCT453, HCT454, HCT455, HCT456, HCT457, HCT458, HCT459, HCT460, HCT461, HCT462, HCT463, HCT464, HCT465, HCT466, HCT467, HCT468, HCT469, HCT470, HCT471, HCT472, HCT473, HCT474, HCT475, HCT476, HCT477, HCT478, HCT479, HCT480, HCT481, HCT482, HCT483, HCT484, HCT485, HCT486, HCT487, HCT488, HCT489, HCT490, HCT491, HCT492, HCT493, HCT494, HCT495, HCT496, HCT497, HCT498, HCT499, HCT500, HCT501, HCT502, HCT503, HCT504, HCT505, HCT506, HCT507, HCT508, HCT509, HCT510, HCT511, HCT512, HCT513, HCT514, HCT515, HCT516, HCT517, HCT518, HCT519, HCT520, HCT521, HCT522, HCT523, HCT524, HCT525, HCT526, HCT527, HCT528, HCT529, HCT530, HCT531, HCT532, HCT533, HCT534, HCT535, HCT536, HCT537, HCT538, HCT539, HCT540, HCT541, HCT542, HCT543, HCT544, HCT545, HCT546, HCT547, HCT548, HCT549, HCT550, HCT551, HCT552, HCT553, HCT554, HCT555, HCT556, HCT557, HCT558, HCT559, HCT560, HCT561, HCT562, HCT563, HCT564, HCT565, HCT566, HCT567, HCT568, HCT569, HCT570, HCT571, HCT572, HCT573, HCT574, HCT575, HCT576, HCT577, HCT578, HCT579, HCT580, HCT581, HCT582, HCT583, HCT584, HCT585, HCT586, HCT587, HCT588, HCT589, HCT590, HCT591, HCT592, HCT593, HCT594, HCT595, HCT596, HCT597, HCT598, HCT599, HCT600, HCT601, HCT602, HCT603, HCT604, HCT605, HCT606, HCT607, HCT608, HCT609, HCT610, HCT611, HCT612, HCT613, HCT614, HCT615, HCT616, HCT617, HCT618, HCT619, HCT620, HCT621, HCT622, HCT623, HCT624, HCT625, HCT626, HCT627, HCT628, HCT629, HCT630, HCT631, HCT632, HCT633, HCT634, HCT635, HCT636, HCT637, HCT638, HCT639, HCT640, HCT641, HCT642, HCT643, HCT644, HCT645, HCT646, HCT647, HCT648, HCT649, HCT650, HCT651, HCT652, HCT653, HCT654, HCT655, HCT656, HCT657, HCT658, HCT659, HCT660, HCT661, HCT662, HCT663, HCT664, HCT665, HCT666, HCT667, HCT668, HCT669, HCT670, HCT671, HCT672, HCT673, HCT674, HCT675, HCT676, HCT677, HCT678, HCT679, HCT680, HCT681, HCT682, HCT683, HCT684, HCT685, HCT686, HCT687, HCT688, HCT689, HCT690, HCT691, HCT692, HCT693, HCT694, HCT695, HCT696, HCT697, HCT698, HCT699, HCT700, HCT701, HCT702, HCT703, HCT704, HCT705, HCT706, HCT707, HCT708, HCT709, HCT710, HCT711, HCT712, HCT713, HCT714, HCT715, HCT716, HCT717, HCT718, HCT719, HCT720, HCT721, HCT722, HCT723, HCT724, HCT725, HCT726, HCT727, HCT728, HCT729, HCT730, HCT731, HCT732, HCT733, HCT734, HCT735, HCT736, HCT737, HCT738, HCT739, HCT740, HCT741, HCT742, HCT743, HCT744, HCT745, HCT746, HCT747, HCT748, HCT749, HCT750, HCT751, HCT752, HCT753, HCT754, HCT755, HCT756, HCT757, HCT758, HCT759, HCT760, HCT761, HCT762, HCT763, HCT764, HCT765, HCT766, HCT767, HCT768, HCT769, HCT770, HCT771, HCT772, HCT773, HCT774, HCT775, HCT776, HCT777, HCT778, HCT779, HCT780, HCT781, HCT782, HCT783, HCT784, HCT785, HCT786, HCT787, HCT788, HCT789, HCT790, HCT791, HCT792, HCT793, HCT794, HCT795, HCT796, HCT797, HCT798, HCT799, HCT800, HCT801, HCT802, HCT803, HCT804, HCT805, HCT806, HCT807, HCT808, HCT809, HCT810, HCT811, HCT812, HCT813, HCT814, HCT815, HCT816, HCT817, HCT818, HCT819, HCT820, HCT821, HCT822, HCT823, HCT824, HCT825, HCT826, HCT827, HCT828, HCT829, HCT830, HCT831, HCT832, HCT833, HCT834, HCT835, HCT836, HCT837, HCT838, HCT839, HCT840,



## pp 7347–7357


A novel series of 1,2,4-triazolo[4,3-*c*]pyrimidine and 1,2,4-triazolo[1,5-*c*]pyrimidine derivatives were prepared, and their Syk family kinase inhibitory activities were assessed.

**pp 7358–7370**

**9**

**pp 7371–7376**

**KT - polysaccharides**



**TSP**  
**HEC**  
**HA**

$[A]_{TSP} > [A]_{HEC} > [A]_{HA}$

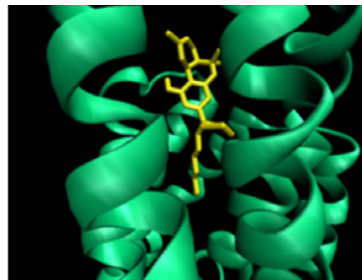
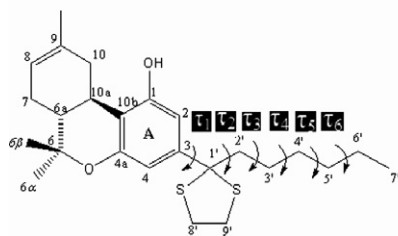
Nuclear magnetic resonance (NMR) spectroscopy demonstrated that, in aqueous solution, ketotifen fumarate bound more strongly to tamarind seed polysaccharide (TSP) than to hydroxyethylcellulose or hyaluronic acid. Results were confirmed by dynamic dialysis technique.



### Comparative molecular dynamics simulations of the potent synthetic classical cannabinoid ligand AMG3 in solution and at binding site of the CB1 and CB2 receptors

pp 7377–7387

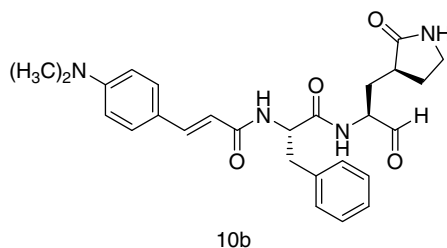
Serdar Durdagi, Heribert Reis, Manthos G. Papadopoulos, Thomas Mavromoustakos\*



### Design, synthesis, and evaluation of 3C protease inhibitors as anti-enterovirus 71 agents

pp 7388–7398

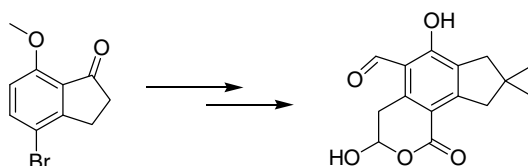
Chih-Jung Kuo, Jiun-Jie Shie, Jim-Min Fang\*, Guei-Rung Yen, John T.-A. Hsu, Hun-Ge Liu, Sung-Nain Tseng, Shih-Cheng Chang, Ching-Yin Lee, Shin-Ru Shih, Po-Huang Liang\*



### Illudalic acid as a potential LAR inhibitor: Synthesis, SAR, and preliminary studies on the mechanism of action

pp 7399–7409

Qing Ling, Yue Huang, Yueyang Zhou, Zhengliang Cai, Bing Xiong, Yahui Zhang, Lanping Ma, Xin Wang, Xin Li, Jia Li\*, Jingkang Shen\*

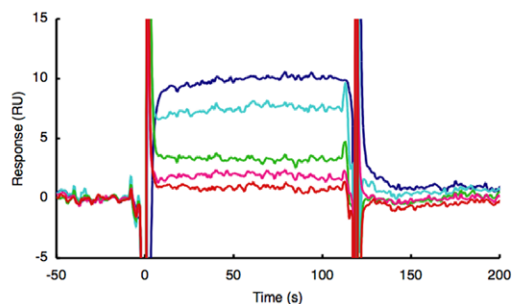
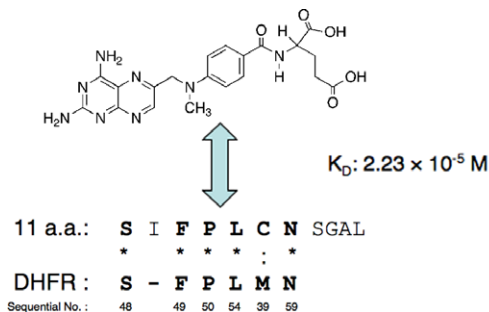


A novel synthesis of the human leukocyte common antigen-related phosphatase (LAR) inhibitor, illudalic acid, has been achieved by a route more amenable to structure modifications. A preliminary study of the structure–activity relationship (SAR) and of the mechanism of action of illudalic acid was conducted.

### Identification of a methotrexate-binding peptide from a T7 phage display screen using a QCM device

pp 7410–7414

Yoichi Takakusagi, Yuki Kuroiwa, Fumio Sugawara\*, Kengo Sakaguchi\*

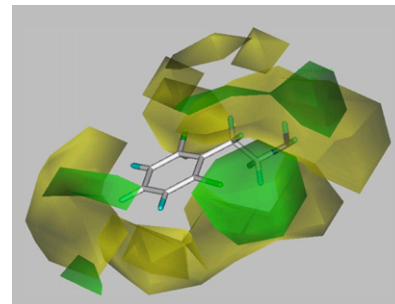


**Structure–activity correlations for  $\beta$ -phenethylamines at human trace amine receptor 1**

pp 7415–7423

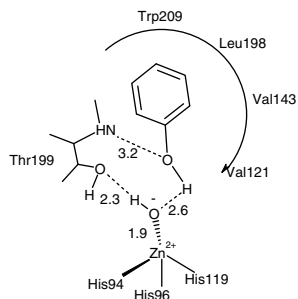
Anita H. Lewin\*, Hernán A. Navarro, S. Wayne Mascarella

CoMFA 3D-QSAR studies on the potency of 68  $\beta$ -phenethylamine analogs to activate hTAAR 1 (61% steric, 39% electrostatic) indicates that bulk both at nitrogen and 4-aryl leads to lower potency.

**Carbonic anhydrase inhibitors: Inhibition of mammalian isoforms I–XIV with a series of substituted phenols including paracetamol and salicylic acid**

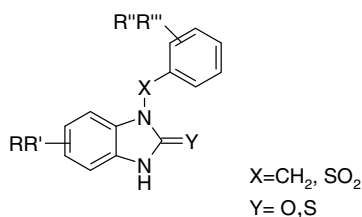
pp 7424–7428

Alessio Innocenti, Daniela Vullo, Andrea Scozzafava, Claudiu T. Supuran\*

**Novel  $N_1$ -substituted 1,3-dihydro-2H-benzimidazol-2-ones as potent non-nucleoside reverse transcriptase inhibitors**

pp 7429–7435

Anna-Maria Monforte\*, Angela Rao, Patrizia Logoteta, Stefania Ferro, Laura De Luca, Maria Letizia Barreca, Nunzio Iraci, Giovanni Maga, Erik De Clercq, Christophe Pannecouque, Alba Chimiri

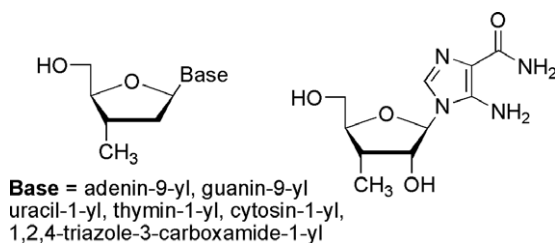


Novel  $N_1$ -substituted 1,3-dihydro-2H-benzimidazol-2-ones were prepared and evaluated as anti-HIV agents. Synthesis and structure–activity relationships are discussed.

**Synthesis of 3'-deoxy-3'-C-methyl nucleoside derivatives**

pp 7436–7442

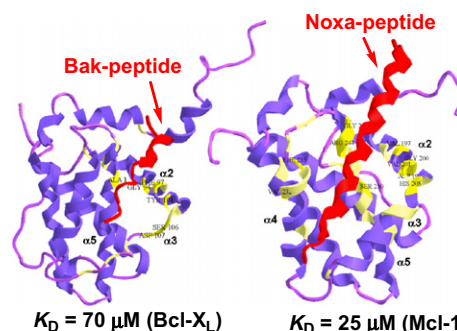
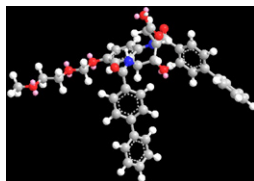
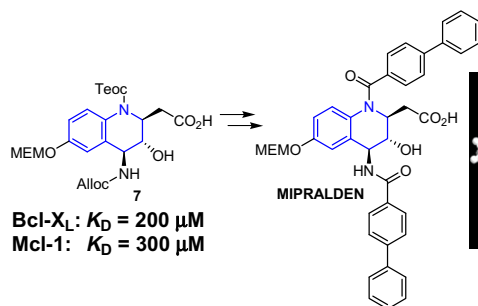
Mohamed Aljarah, Sarah Couturier, Christophe Mathé, Christian Périgaud\*



**The discovery of small molecule chemical probes of Bcl-X<sub>L</sub> and Mcl-1**

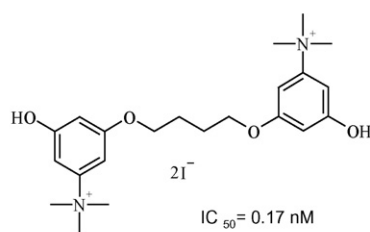
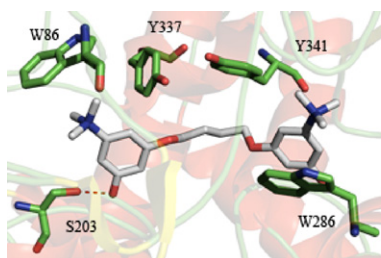
pp 7443–7449

Michael Prakesch, Alexey Yu Denisov, Marwen Naim, Kalle Gehring\*, Prabhat Arya\*

**Homo- and hetero-bivalent edrophonium-like ammonium salts as highly potent, dual binding site AChE inhibitors**

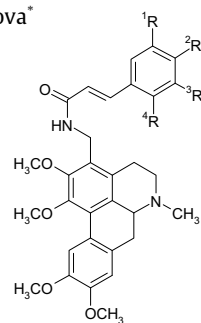
pp 7450–7456

Francesco Leonetti, Marco Catto, Orazio Nicolotti, Leonardo Pisani, Anna Cappa, Angela Stefanachi, Angelo Carotti\*

**Cinnamoyl- and hydroxycinnamoyl amides of glucine and their antioxidative and antiviral activities**

pp 7457–7461

Maya Spasova, Stefan Philipov, L. Nikolaeva-Glomb, A. S. Galabov, Ts. Milkova\*

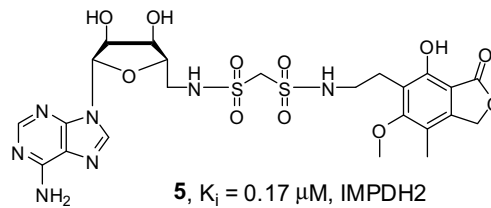
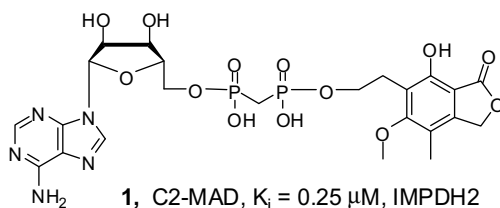


Cinnamoyl-, feruloyl-, sinapoyl-, *o*-, and *p*-coumaroyl amides of 3-aminomethylglucine were synthesized, and their antiviral activity and antioxidant potential against DPPH\* test were estimated.

**Bis(sulfonamide) isosters of mycophenolic adenine dinucleotide analogues: Inhibition of inosine monophosphate dehydrogenase**

pp 7462–7469

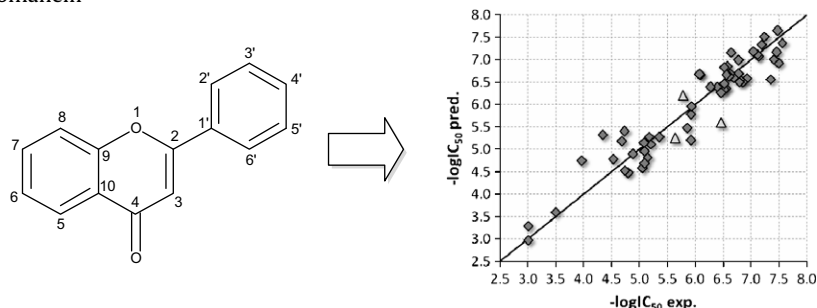
Liqiang Chen, Riccardo Petrelli, Magdalena Olesiak, Daniel J. Wilson, Nicholas P. Labello, Krzysztof W. Pankiewicz\*



**QSAR prediction of inhibition of aldose reductase for flavonoids**

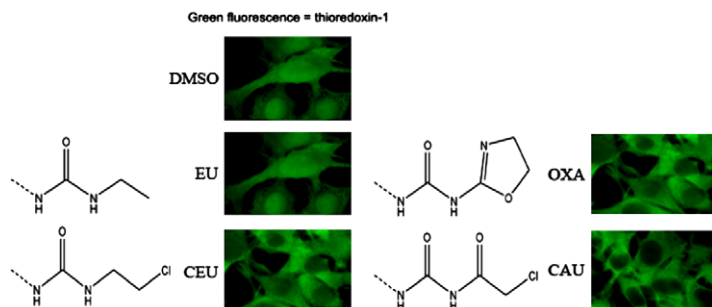
pp 7470–7476

Andrew G. Mercader\*, Pablo R. Duchowicz, Francisco M. Fernández, Eduardo A. Castro, Daniel O. Bennardi, Juan C. Autino, Gustavo P. Romanelli

**Aromatic 2-chloroethyl urea derivatives and bioisosteres. Part 2: Cytocidal activity and effects on the nuclear translocation of thioredoxin-1, and the cell cycle progression**

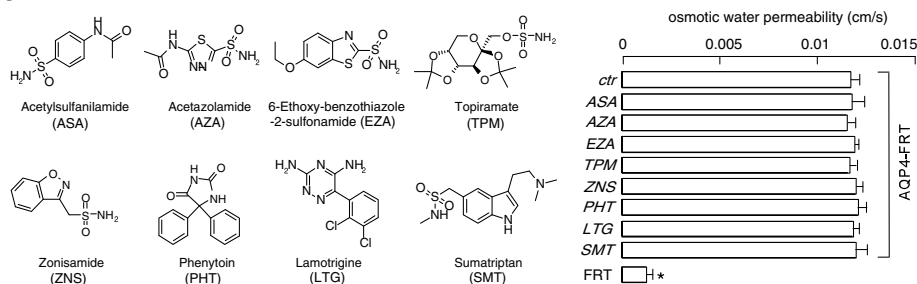
pp 7477–7488

Jessica S. Fortin\*, Marie-France Côté, Jacques Lacroix, Éric Petitclerc, René C.-Gaudreault\*

**Lack of aquaporin-4 water transport inhibition by antiepileptics and arylsulfonamides**

pp 7489–7493

Baoxue Yang, Hua Zhang, A. S. Verkman\*

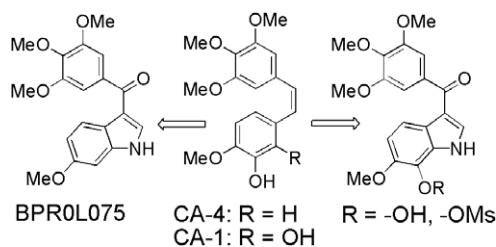


Several antiepileptics, arylsulfonamides, and related small molecules were tested for their ability to inhibit brain water channel AQP4. Multiple functional assays showed no inhibition by these compounds.

**Synthesis and biological evaluation of new disubstituted analogues of 6-methoxy-3-(3',4',5'-trimethoxybenzoyl)-1H-indole (BPR0L075), as potential antivascular agents**

pp 7494–7503

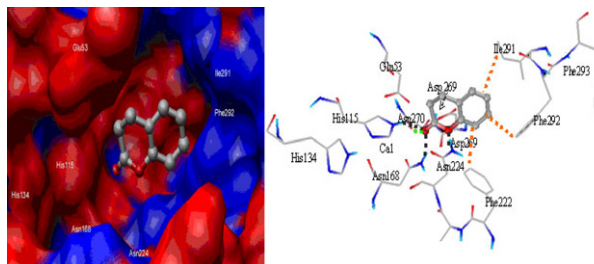
Nancy Ty, Grégory Dupeyre, Guy G. Chabot, Johanne Seguin, François Tillequin, Daniel Scherman, Sylvie Michel\*, Xavier Cachet\*



**Characterization of the PON1 active site using modeling simulation, in relation to PON1 lactonase activity**

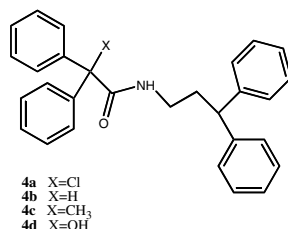
pp 7504–7509

Hagai Tavori, Soliman Khatib, Michael Aviram, Jacob Vaya\*

**Novel sterically hindered cannabinoid CB<sub>1</sub> receptor ligands**

pp 7510–7515

Paolo Urbani, Maria Grazia Cascio, Anna Ramunno, Tiziana Bisogno, Carmela Saturnino, Vincenzo Di Marzo\*

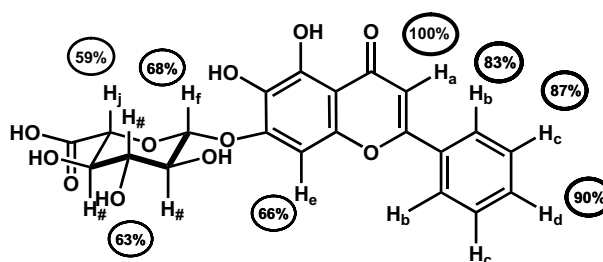


Eleven novel *N*-(3,3-diphenyl)propyl-2,2-diphenylacetamide derivatives and six triphenylacetamides were synthesized and tested as ligands of cannabinoid CB<sub>1</sub> and CB<sub>2</sub> receptors. Compound **4b** was the most potent CB<sub>1</sub> ligand.

**Baicalin, a prodrug able to reach the CNS, is a prollyl oligopeptidase inhibitor**

pp 7516–7524

Teresa Tarragó, Nessim Kichik, Birgit Claasen, Roger Prades, Meritxell Teixidó, Ernest Giralt\*

**OTHER CONTENTS****Instructions to contributors**

p I

\*Corresponding author

Supplementary data available via ScienceDirect

**COVER**

An insight into biologically relevant chemical space showing the scaffolds of potential natural-product based inhibitors orbiting their target, the protein structure of protein 11-beta steroid dehydrogenase (PDB code 1xu7). Graphic produced using Pymol (<http://www.pymol.org>). [M. A. Koch, A. Schuffenhauer, M. Scheck, S. Wetzel, M. Casaulta, A. Odermatt, P. Ertl, H. Waldmann, Charting biologically relevant chemical space: A structural classification of natural products (SCONP), *PNAS* **2005**, 102, 17272–17277 and S. Wetzel, H. Waldmann, Cheminformatic analysis of natural products and their chemical space, *Chimia* **2007**, 61(6), 355–360].

---

Available online at  
 **ScienceDirect**  
[www.sciencedirect.com](http://www.sciencedirect.com)

---

Indexed/Abstracted in: Beilstein, Biochemistry & Biophysics Citation Index, CANCERLIT, Chemical Abstracts, Chemistry Citation Index, Current Awareness in Biological Sciences/BIOBASE, Current Contents: Life Sciences, EMBASE/Excerpta Medica, MEDLINE, PASCAL, Research Alert, Science Citation Index, SciSearch, TOXFILE

---

**ELSEVIER**

ISSN 0968-0896